Localization and function of a calmodulin–apocalmodulin-binding domain in the N-terminal part of the type 1 inositol 1,4,5-trisphosphate receptor

Ilse SIENAERT[1,2], Nael NADIF KASRI[2], Sara VANLINGEN, Jan B. PARYS, Geert CALLEWAERT, Ludwig MISSIAEN and Humbert DE SMEDT

Laboratorium voor Fysiologie, Katholieke Universiteit Leuven Campus Gasthuisberg O/N, Herestraat 49, B-3000 Leuven, Belgium

Calmodulin (CaM) is a ubiquitous protein that plays a critical role in regulating cellular functions by altering the activity of a large number of proteins, including the D-*myo*-inositol 1,4,5-trisphosphate (IP_3) receptor (IP_3R). CaM inhibits IP_3 binding in both the presence and absence of Ca^{2+} and IP_3-induced Ca^{2+} release in the presence of Ca^{2+}. We have now mapped and characterized a Ca^{2+}-independent CaM-binding site in the N-terminal part of the type 1 IP_3R (IP_3R1). This site could be responsible for the inhibitory effects of CaM on IP_3 binding. We therefore expressed the N-terminal 581 amino acids of IP_3R1 as a His-tagged recombinant protein, containing the functional IP_3-binding pocket. We showed that CaM, both in the presence and absence of Ca^{2+}, inhibited IP_3 binding to this recombinant protein with an IC_{50} of approx. 2 μM. Deletion of the N-terminal 225 amino acids completely abolished the effects of both Ca^{2+} and CaM on IP_3 binding. We mapped the Ca^{2+}-independent CaM-binding site to a recombinant glutathione S-transferase fusion protein containing the first 159 amino acids of IP_3R1 and then made different synthetic peptides overlapping this region. We demonstrated that two synthetic peptides matching amino acids 49–81 and 106–128 bound CaM independently of Ca^{2+} and could reverse the inhibition of IP_3 binding caused by CaM. This suggests that these sequences are components of a discontinuous Ca^{2+}-independent CaM-binding domain, which is probably involved in the inhibition of IP_3 binding by CaM.

Key words: calcium signalling, inositol 1,4,5-trisphosphate (IP_3), synthetic peptide.

INTRODUCTION

Calmodulin (CaM) is a ubiquitous cytosolic protein that plays a critical role in regulating cellular functions by altering the activity of a large number of proteins, in particular the intracellular Ca^{2+}-release channels. This has recently [1–5] been well documented for the ryanodine receptor family. CaM also interacts with all three isoforms of the D-*myo*-inositol 1,4,5-trisphosphate (IP_3) receptor (IP_3R), both in a Ca^{2+}-dependent and a Ca^{2+}-independent way. All functional data on full-length IP_3Rs report inhibition of IP_3-induced Ca^{2+} release by CaM [6–10]. Inhibition occurred only in the presence of Ca^{2+} (≥ 0.1 μM) [7–10]. Reconstitution experiments, in which purified cerebellar type 1 IP_3R (IP_3R1) was converted into lipid bilayers, showed that channel activity was inhibited by > 1 μM concentrations of Ca^{2+} only after addition of CaM [11]. Besides an inhibitory effect on IP_3-induced Ca^{2+} release in the presence of Ca^{2+}, CaM was also reported to cause a Ca^{2+}-independent inhibition of IP_3 binding to full-length IP_3R1 [6,12–14], but not to IP_3R3 [12]. Binding of IP_3 to a recombinant ligand-binding domain, however, was inhibited by exogenous CaM for all the three IP_3R isoforms [15]. Taken together, these results clearly demonstrated that CaM inhibits the IP_3R function for all IP_3R isoforms.

Amino acids 1565–1586 in the regulatory domain of IP_3R1 have long been considered as the only CaM interaction site, which is also conserved in IP_3R2 but not in IP_3R3 [16]. The mutation of tryptophan to alanine (W1577A) within this site eliminated CaM binding [16], but surprisingly did not alter the Ca^{2+} regulation of the IP_3R [14]. Recently [7], binding of CaM has been demonstrated by a sensitive scintillation-proximity assay in two regions of IP_3R1. These were localized in the N-terminal part (amino acids 1–159) and in a cytosolic region (amino acids 1499–1649) encompassing the Ca^{2+}-dependent CaM-binding site of amino acids 1565–1586 [7]. An additional CaM-binding site is created by alternative splicing of IP_3R1, due to the deletion of the S2 region (amino acids 1693–1733) [17,18].

However, it is not clear whether the observed binding sites are related to the inhibitory function of CaM on either Ca^{2+} release or IP_3 binding. In the present study, we have made a detailed analysis of the interaction of CaM with the IP_3-binding domain of IP_3R1. We characterized the effects of Ca^{2+} and CaM on [^{3}H]IP_3 binding using recombinant ligand-binding domains and mutants thereof. We now demonstrate that CaM binds with micromolar affinity to the first 159 amino acids of IP_3R1, both in the absence and presence of Ca^{2+}. Furthermore, two synthetic peptides that matched amino acids 49–81 and 106–128 bound CaM independently of Ca^{2+} and could reverse the CaM-induced inhibition of IP_3 binding to the recombinant ligand-binding domain and to the full-size IP_3R1. These results suggest that the sequences are components of a discontinuous Ca^{2+}-independent CaM-binding domain and might be responsible for the inhibition of IP_3 binding.

MATERIALS AND METHODS

cDNA construction and site-directed mutagenesis

The cDNA encoding the N-terminal 581 amino acids of the mouse IP_3R1 was amplified by PCR and cloned into the *Nde*I–*Xho*I site of the pET21b/+ vector (Novagen), yielding

Abbreviations used: CaM, calmodulin; dCaM, dansyl-calmodulin; DDT, 1,1,1-trichloro-2,2-bis-(*p*-chlorophenyl)ethane; IP_3, D-*myo*-inositol 1,4,5-trisphosphate; IP_3R, IP_3 receptor; GST, glutathione S-transferase; Ni-NTA, nickel-nitrilotriacetic acid; pGST, parental GST.

[1] To whom correspondence should be addressed (e-mail Ilse.Sienaert@med.kuleuven.ac.be).

[2] Both authors contributed equally to the present study.

pET-581/1His, to obtain the N-terminal 581 amino acids of the mouse IP_3R1 with a 6× His-tagged C-terminus (Lbs-1His).

The plasmid expressing the N-terminal deletion mutant (Lbs-1His Δ1–225) was produced by PCR, with forward-primer 5′-GGCAGGCATATGTGGAGTGATAACAAAGACG-3′ and reverse-primer 5′-GGATCTCAGTGGTGGTGG-3′, by using pET-581/1His as a template. The forward primer contained the site for *Nde*I (CATATG) in frame at the corresponding position to introduce a new start codon (Met) as a substitute for Lys-224.

Site-directed mutagenesis was performed by using the QuickChange point-mutation kit (Stratagene, La Jolla, CA, U.S.A.). Briefly, forward primers were designed according to the manufacturer's recommendation as follows: E425A,D426A 5′-CCTCTCCCCTGAAGGCGGCCAAGGAAGCATTTGCC-3′; E428A 5′-CCCCTGAAGGCGGCC AAGGCAGCATTTGCCATAG-3′; D442A,D444A 5′-CCCCTGCTGAGGTTCGGGCCCTGGCCTTTGCCAATG-3′. Reverse primers were the complementary sequence of the forward primers. PCR conditions, parental template digestion and transformation into *Escherichia coli* strain DH5α were performed according to the manufacturer's instructions. Primers E425A,D426A, E428A and D442A,D444A were sequentially used to obtain a plasmid (pET-581/1His mut5) encoding the N-terminal 581 amino acids of the mouse IP_3R1 with 5-point mutations (Lbs-1His mut5). The same mutations were introduced in pGEX-2T-Cyt3b [19], yielding mutant fusion protein GST-Cyt3b mut5 (GST, glutathione S-transferase). All constructs were sequenced to confirm mutations.

Expression in *E. coli*, preparation of the soluble fraction and purification of Lbs-1His domains

The expression of the N-terminal 581 amino acids of the IP_3R1 constructs (Lbs-1His, Lbs-1His mut5 and Lbs-1His Δ1–225) was essentially as described by Sipma et al. [13]. Preparation of the soluble fraction of *E. coli* was performed according to the manufacturer's recommendations (Qiaexpressionist, Qiagen). Briefly, cell pellets were resuspended in 7 ml of lysis buffer [50 mM NaH_2PO_4 (pH 7.0)/300 mM NaCl/10 mM imidazole/1 mM β-mercaptoethanol/0.8 mM benzamidine/0.2 mM PMSF/10 μM leupeptin/1 μM pepstatin A/75 nM aprotinin]. This cell suspension was digested with lysozyme (0.1 mg/ml) for 30 min at 4 °C, followed by 6 cycles of freeze–thawing and sonication at 12 kHz, twice for 15 s. After centrifugation at 30000 ***g*** for 60 min at 4 °C, the supernatant was collected for purification. His-tag purification of the clear lysate (4 ml) was performed by adding 1 ml of 50 % (v/v) nickel-nitrilotriacetic acid (Ni-NTA; Qiagen). The lysate–Ni-NTA mixture was gently mixed at 4 °C for 60 min, loaded on to a column and was washed with 2 vol. of lysis buffer supplemented with 10 mM imidazole. Finally, the recombinant protein was eluted with 0.5 ml of 4× elution buffer (= lysis buffer containing 250 mM imidazole). The protein was eluted in the second and third fractions.

[^{3}H]IP_3 binding

Binding studies were performed as described previously [13]. [^{3}H]IP_3 binding was performed at 0 °C in a 100 μl of binding buffer containing 50 mM Tris/HCl (pH 7.0), 1 mM EGTA and 10 mM β-mercaptoethanol. Free Ca^{2+} concentration was calculated using the CaBuf program (available at ftp.cc.kuleuven.ac.be/pub/droogmans/cabuf.zip) and based on the stability constants given by Fabiato and Fabiato [20]. After 30 min of incubation, 10 μl of γ-globulin (20 mg/ml) and 110 μl of 20 % (w/v) poly(ethylene glycol) in IP_3-binding solution were added and the samples were rapidly passed through glass fibre filters. The amount of purified protein used for each reaction ranged between 1.5 and 3.5 μg. Non-specific binding was determined in the presence of 12.5 μM unlabelled IP_3.

Expression and purification of CaM and CaM1234

The mammalian CaM cDNA was provided by Dr Z. Grabarek (Boston Biomedical Institute, Boston, MA, U.S.A.) [21] and the rat cDNA for CaM1234 by Dr J. Adelman (Oregon Health Science University, Portland, OR, U.S.A.). The coding sequence of CaM1234 was amplified by PCR and subcloned into the *Nde*I and *Bam*HI sites of pET21b vector (Novagen).

The expression vectors pAED4 and pET21b, containing wild-type CaM and CaM1234 respectively, were transformed into BL21 *E. coli*, grown to mid-exponential phase and induced with 0.3 mM isopropyl-1-thio-β-D-galactopyranoside either for 2 h at 37 °C (CaM) or for 4 h at 28 °C (CaM1234). The cells were lysed by three rapid cycles of freeze–thawing between liquid nitrogen and 37 °C, or by sonication at 20 kHz, nine times for 20 s using a probe sonicator (MSE Ltd, Crawley, Surrey, U.K.) in a buffer containing 50 mM Tris/HCl (pH 7.4), 2 mM EDTA, 1 mM 1,1,1-trichloro-2,2-bis-(*p*-chlorophenyl)ethane (DDT), 0.8 mM benzamidine, 0.2 mM PMSF, 10 μM leupeptin, 1 μM pepstatin and 75 nM aprotinin. The lysate was cleared by ultra-centrifugation at 140000 ***g*** for 30 min at 4 °C. Before heating, NaCl and $CaCl_2$ were added to the CaM supernatant to a final concentration of 500 and 50 mM respectively. The NaCl concentration in the CaM1234 supernatant was brought to 150 mM. The lysate was heated to 70 °C, immediately cooled on ice and centrifuged at 140000 ***g*** for 30 min at 4 °C. The wild-type CaM supernatant was applied to a phenyl-Sepharose column in the presence of Ca^{2+} [equilibration buffer: 50 mM Tris/HCl (pH 7.4), 5 mM $CaCl_2$, 1 mM DDT, 0.1 M NaCl]. The column was subsequently washed with buffer A [50 mM Tris/HCl (pH 7.4), 0.1 mM $CaCl_2$, 1 mM DDT] and buffer B [50 mM Tris/HCl (pH 7.4), 0.1 mM $CaCl_2$, 1 mM DDT, 0.5 M NaCl]. Finally, CaM was eluted with 50 mM Tris/HCl (pH 7.4), 5 mM EGTA and 1 mM DDT. The CaM1234 supernatant was filtered and concentrated using Centriprep YM-30 (1500 ***g*** for 45 min at 4 °C); the filtrate was transferred to Centriprep YM-10 and further concentrated until the volume of non-diffusible material was < 2 ml. The non-diffusible material was further concentrated in Centricon-10. The purity of CaM and CaM1234 was verified by SDS/PAGE and final protein concentrations were determined by the Lowry procedure [22].

Fluorescence assay for binding dansyl-CaM (dCaM)

Dansylation of CaM was performed according to the manufacturer's recommendations (Molecular Probes, Eugene, OR, U.S.A.). Binding experiments were performed as described by Lin et al. [18]. Emission spectra were measured between 400 and 600 nm after excitation at 340 nm with an Aminco–Bowman Series 2 Spectrofluorimeter (Spectronic Instruments, NY, U.S.A.). The buffer used contained 20 mM Tris/HCl (pH 8.0), 250 mM NaCl, 5 mM $MgCl_2$ and 100 μM EGTA. We have also verified that essentially the same results were obtained at pH 7.0 (results not shown).

Interactions between CaM1234 and GST-fusion proteins

Expression and purification of GST-fusion proteins were performed as described previously [19,23]. For binding experiments between GST-fusion proteins and CaM1234, the GST-fusion

protein supernatant was incubated overnight with glutathione–Sepharose 4B beads at 4 °C and washed extensively with a buffer containing 150 mM NaCl, 50 mM Tris/HCl (pH 7.4), 0.1 % (v/v) Triton X-100 (binding buffer) and the indicated amount of free Ca^{2+}. CaM1234 (approx. 30 μg/reaction) was then added and allowed to interact with the fusion protein (approx. 20 μg/reaction) for 4 h at 4 °C. The beads were then washed extensively with a binding buffer containing the indicated amounts of free Ca^{2+} and the retained protein eluted with the SDS sample buffer. The protein was subjected to SDS/PAGE, transferred to Immobilon P (Millipore Corporation, Bedford, MA, U.S.A.) and detected by immunoblot with a polyclonal antibody raised against CaM (dilution 1:1000; Zymed Laboratories, San Francisco, CA, U.S.A.). This antibody is competent in detecting both CaM1234 and CaM [24]. Immunodetection was exactly as described previously [25]. Free Ca^{2+} concentration buffered with EGTA was calculated by the CaBuf program.

Non-denaturing gel electrophoresis

The electrophoretic mobility of CaM or CaM1234 was evaluated by non-denaturing discontinuous PAGE as described by Laemmli [26]. Non-denaturing gels (15 % polyacrylamide) were run at 25 mA at 4 °C under high Ca^{2+} conditions (200 μM free Ca^{2+} in all gel buffers) or low Ca^{2+} conditions (1 mM EGTA in all gel buffers).

RESULTS

Expression of the ligand-binding domain of IP_3R1 (Lbs-1His), a point mutant Lbs-1His mut5 and a deletion mutant Lbs-1His Δ1–225

The amino acid boundaries of the Lbs-1His, Lbs-1His mut5 and Lbs-1HisΔ1–225 constructs together with the position of the mutations are schematically shown in Figure 1(A). We constructed a bacterial expression vector encoding the N-terminal 581 amino acids of mouse IP_3R1 with a C-terminal His-tag. The resulting recombinant protein was expressed in *E. coli* and affinity-purified on an Ni-NTA column. It migrated with an apparent molecular mass of 66 kDa, as determined by SYPRO Orange™ staining after SDS/PAGE (Figure 1B, right panel) and Western blotting using an anti-His antibody (Figure 1B, left panel). The ligand-binding properties of Lbs-1His were essentially the same (results not shown) as described previously for Lbs-1 without a His-tag [13].

In the earlier studies on Lbs-1, it was found that both Ca^{2+} and CaM reduced the binding of IP_3 [13]. We developed different mutated Lbs-1His constructs to discriminate between both effects. Since Lbs-1 contains two amino acid sequences (Cyt3a, 304–381; Cyt3b, 378–450) that were found to bind Ca^{2+} [19], we investigated whether these sites could be involved in the inhibitory effect of Ca^{2+}. Since the pattern of Asp and Glu residues is fully conserved over the three IP_3R isoforms in stretch 378–450 (Cyt3b), we constructed a mutant ligand-binding domain in which five negatively charged amino acids were mutated to Ala: Glu-425, Asp-426, Glu-428, Asp-442 and Asp-444. The resulting recombinant protein (Lbs-1His mut5) expressed in *E. coli* and affinity-purified on an Ni-NTA column, also migrated with an apparent molecular mass of 66 kDa (Figure 1B). The mutant Lbs-1His mut5 specifically bound [^{3}H]IP_3 at pH 7.0, although a 2–3-fold decrease in specific IP_3-binding activity was observed compared with Lbs-1His (results not shown). Introduction of the mutations resulted in a ligand-binding site with no Ca^{2+}-binding capacity in the 378–450 amino acid stretch. This was verified by performing the same mutagenesis on the GST-fusion protein GST-Cyt3b, which resulted in a complete loss of Ca^{2+} binding as determined by $^{45}Ca^{2+}$ overlay (results not shown).

To demonstrate a functional interaction of CaM with the N-terminal region (amino acids 1–159) of IP_3R1 [6,7,12,13], we constructed a deletion mutant of the ligand-binding domain. To maintain IP_3 binding, we had to preserve amino acids 226–578 of the ligand-binding site, as described by Yoshikawa et al. [27]. The resulting recombinant protein (Lbs-1His Δ1–225) expressed in *E. coli* and affinity-purified on an Ni-NTA column, migrated with an apparent molecular mass of 42 kDa (Figure 1B, lane 3). However, some contaminating proteins were co-purified as visualized by SYPRO Orange™ (Figure 1B, right panel, lane 3). The Δ1–225 mutant showed binding specificity similar to that of Lbs-1His (results not shown).

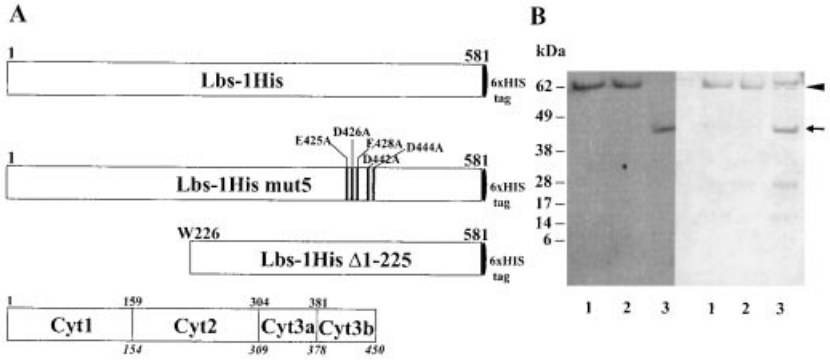

Figure 1 Characteristics of the recombinant ligand-binding domains and GST-fusion proteins

(**A**) Schematic diagram of the boundaries of the His-tagged IP_3R1 ligand-binding domain Lbs-1His. The positions of the point mutations in Lbs-1His mut5 and the deletion mutant Lbs-1His Δ1–225 constructed in the present study are indicated. Also shown are the boundaries of the GST-fusion proteins GST-Cyt1, -2, -3a and -3b constructed in previous studies [19]. GST-Cyt3a and -3b represent two putative Ca^{2+}-binding sites (amino acids 304–381 and 378–450). The numbering of the amino acids corresponds to the mouse cDNA clone [49]. (**B**) Affinity-purified soluble fraction of *E. coli* (2 μg/lane) transformed with pET-581/1His (lane 1), pET-581/1His mut5 (lane 2) or with pET-581/1His Δ1–225 (lane 3) were separated by SDS/PAGE (4–12% Bis-Tris gel; NuPage®) and either transferred to Immobilon-P and probed with mouse anti-His (1:1000) (left panel) or stained with SYPRO Orange (right panel). The positions of Lbs1-His, Lbs-1His mut5 (arrowhead) and Lbs1-His Δ1–225 (arrow) are indicated.

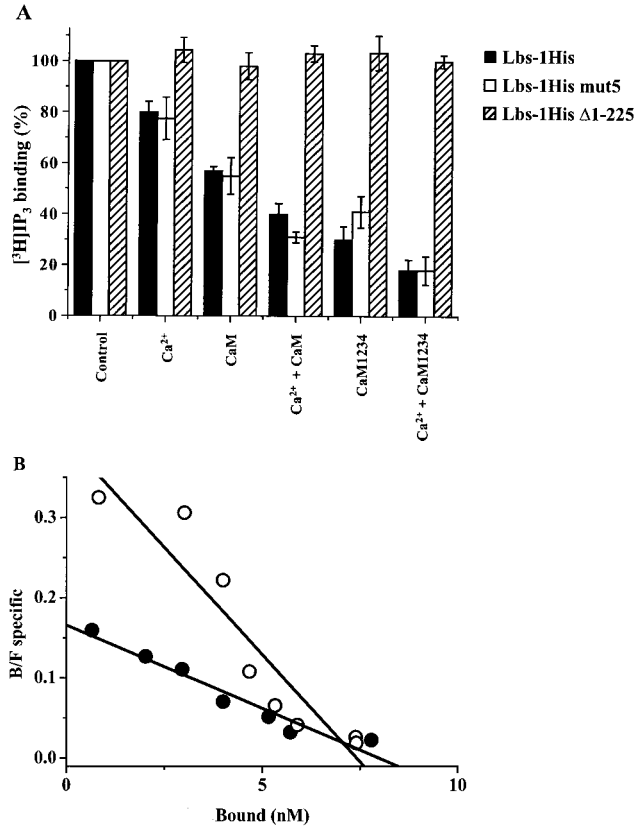

Figure 2 Effect of Ca^{2+}, CaM and CaM1234 on binding to Lbs-1His, Lbs-1His mut5 and Lbs-1His Δ1–225

(**A**) [^{3}H]IP_3 binding to IP_3-binding proteins purified on Ni-NTA (Lbs-1His, Lbs-1His mut5 and Lbs-1His Δ1–225) was measured in the presence and absence of Ca^{2+} (5 μM) and/or CaM/CaM1234 (10 μM) and is expressed as the percentage in the absence of these modulators (control). Binding was measured at pH 7.0 in the presence of 1 mM EGTA and 3.5 nM [^{3}H]IP_3. Data are expressed as the means ± S.E.M. of at least three experiments, consisting of independent triplicates. (**B**) A Scatchard analysis of IP_3 binding to Lbs-1His in the presence and absence of CaM is presented. Affinity-purified Lbs-1His (1.5 μg) was incubated with 3.5 nM [^{3}H]IP_3 at pH 7.0 and increasing concentrations of unlabelled IP_3 in the absence (○) or presence (●) of 10 μM CaM. Data are expressed as means of two independent determinations, consisting of independent quadruplicates.

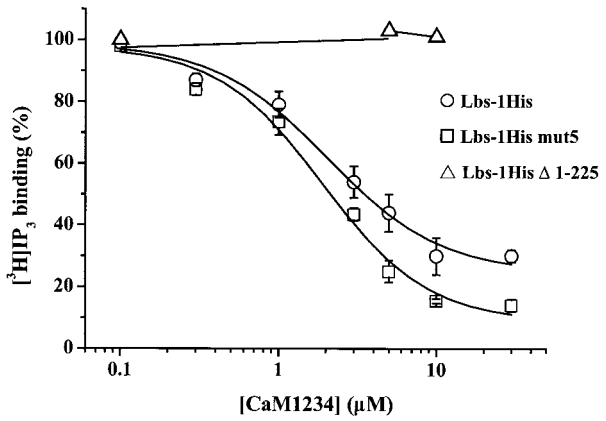

Figure 3 Effect of different CaM1234 concentrations on IP_3 binding to Lbs-1His, Lbs-1His mut5 and Lbs-1His Δ1–225

[^{3}H]IP_3 binding to purified Lbs-1His (○), Lbs-1His mut5 (□) and Lbs-1His Δ1–225 (△) in the presence of indicated concentrations of CaM1234 was expressed as a percentage of the binding measured in Ca^{2+}-free buffer (1 mM EGTA, pH 7.0) without CaM1234. Curve fitting was done by Microcal™ Origin Version 6.0 (Northampton, MA, U.S.A.) and yielded a K_i value of approx. 2.0 μM for Lbs-1His and approx. 1.9 μM for Lbs-1His mut5. Data are expressed as the means ± S.E.M. of at least three experiments, consisting of independent triplicates.

Effect of CaM and CaM1234 on IP_3 binding to Lbs-1His, Lbs-1His mut5 and Lbs-1His Δ1–225 in the absence and presence of Ca^{2+}

Micromolar free Ca^{2+} concentrations (5 μM) inhibited IP_3 binding to Lbs-1His by 20.0 ± 4.2 % at a physiological pH of 7.0 (Figure 2A). Surprisingly, IP_3 binding to Lbs-1His mut5 was inhibited to the same extent by 5 μM Ca^{2+} under identical conditions (22.5 ± 8.3 %; Figure 2A), and deletion of the first N-terminal 225 amino acids (Lbs-1His Δ1–225) abolished the inhibition by Ca^{2+}.

CaM (10 μM) inhibited IP_3 binding to Lbs-1His and Lbs-1His mut5 by 43.0 ± 1.7 and 45.0 ± 7.2 % respectively (Figure 2A), whereas no inhibition was observed for Lbs-1His Δ1–225. Scatchard analysis performed in the absence or presence of CaM (10 μM) yielded K_d values of 19 ± 4 and 33 ± 4 nM respectively, whereas B_{max} values were not significantly different (500 ± 25 and 533 ± 32 pmol/mg; Figure 2B). This indicates that CaM reduced the affinity of the IP_3-binding site but did not affect the number of IP_3-binding sites. The B_{max} value is significantly higher than previously published values [13,25,27], which probably reflects a higher degree of purification of our preparation and/or a higher fraction of functionally active recombinant proteins. In the presence of both Ca^{2+} (5 μM) and CaM (10 μM), IP_3 binding was inhibited by 60.0 ± 4.2 % for Lbs-1His and by 69.0 ± 2.1 % for Lbs-1His mut5 (Figure 2A). Inhibition by CaM was fully additive to inhibition by Ca^{2+}, indicating that the inhibition caused by CaM was Ca^{2+}-independent. We have obtained essentially the same results for full-length IP_3R1. Maximal CaM-induced inhibition of IP_3 binding to microsomes of insect Sf9 cells expressing mouse IP_3R1 was approx. 40 % in the absence of Ca^{2+}. This is very close to the value published previously (36 % [13]) and approx. 55 % in the presence of 10 μM Ca^{2+} (results not shown). To exclude the possibility that the observed Ca^{2+}-independent CaM effect was due to a constitutively occupied Ca^{2+}-binding site with a very high Ca^{2+} affinity in the CaM molecule, we used CaM1234, a CaM mutant that could no longer bind Ca^{2+}. CaM1234 (10 μM) inhibited IP_3 binding to Lbs-1His and Lbs-1His mut5 by 70.0 ± 5.3 and 59.0 ± 6.2 % respectively, and no inhibition was observed for Lbs-1His Δ1–225 (Figure 2A). In the presence of both Ca^{2+} (5 μM) and CaM1234 (10 μM), IP_3 binding was further inhibited up to 82.1 ± 4.0 % for both Lbs-1His and 82.1 ± 4.9 % for Lbs-1His mut5. Inhibition by CaM1234 was therefore also additive to inhibition by Ca^{2+} (Figure 2A). Again, we obtained similar results for microsomes of insect Sf9 cells expressing the full-length mouse IP_3R1: maximal CaM1234-induced inhibition of IP_3 binding to full-length IP_3R1 was approx. 37 % in the absence of Ca^{2+} and approx. 47 % in the presence of 10 μM Ca^{2+} (results not shown). The effect of CaM1234 on IP_3 binding to Lbs-1His was concentration-dependent (Figure 3). CaM1234 half-maximally inhibited IP_3 binding at a concentration of approx. 2.0 μM. This value was similar to the one found for Lbs-1His mut5 (1.9 μM). The inhibitory effect of CaM1234 was completely abolished for Lbs-1His Δ1–225.

Binding of CaM to N-terminal fusion proteins of IP_3R1

The IP_3-binding experiments suggest the presence of a functional Ca^{2+}-independent CaM-binding site within the first 225 amino acids of IP_3R1. To demonstrate directly the presence of such a

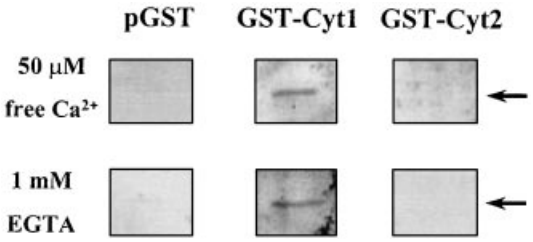

Figure 4 Interaction between CaM1234 and pGST, GST-Cyt1 and GST-Cyt2

Immunoblot showing the interaction of pGST, GST-Cyt1 and GST-Cyt2 with CaM1234 in a pull down assay in the presence (50 μM free Ca^{2+}) and absence of Ca^{2+} (1 mM EGTA). Positive signals on the immunoblot indicate retention of CaM1234 as detected by polyclonal rabbit anti-CaM antibody (dilution 1:1000). pGST was used as negative control. Representative data for four analyses with nearly identical results are shown.

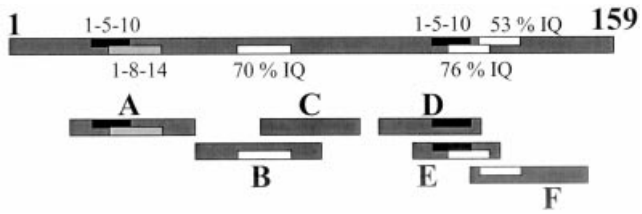

Figure 6 Detailed analysis of CaM-binding properties of the N-terminal 1–159 amino acid region of IP_3R1

Map showing positions of synthetic peptides (A–F) used for binding experiments relative to the N-terminal 159 amino acid region of IP_3R1. Partial consensus domains for CaM binding [35] are indicated.

Ca^{2+}-independent CaM-binding site within this N-terminal region, we first employed a pull down assay between CaM1234 and immobilized GST-fusion proteins GST-Cyt1 (amino acids 1–159) and GST-Cyt2 (amino acids 154–309) that overlap this region [19]. As shown in Figure 4, GST-Cyt1 was able to bind CaM1234 both in the presence and absence of Ca^{2+}. Neither parental GST (pGST) nor GST-Cyt2 showed interaction with CaM1234. We also assayed the interaction with GST-Cyt1 by measuring the fluorescence changes of dCaM. dCaM binding to a CaM-binding protein is known to induce an increase in the emission maximum and a blue shift in the fluorescence spectrum of the dansyl moiety [28]. We observed these changes when GST-Cyt1 was added to a buffer containing dCaM (40 nM) in the presence of Ca^{2+} (Figure 5A) as well as in the presence of an excess of EGTA (Figure 5B). These changes were not observed on addition of pGST as a control (Figure 5C). For both conditions (0.5 mM free Ca^{2+} and 1 mM EGTA), binding of GST-Cyt1 was quantified by measuring the fluorescence increase at 500 nm as a function of increasing concentrations of the GST-fusion protein. The increase in fluorescence was approximately the same in both conditions; when fitted, both curves showed an equilibrium binding to a single site with a similar K_d value of approx. 400 nM (Figure 5D). This confirmed the presence of a low-affinity Ca^{2+}-independent CaM-binding site in the N-terminal 159 amino acids of IP_3R1.

Binding of CaM to IP_3R1 peptides

For a precise identification of the CaM interaction site in the N-terminal 159 amino acid region, we synthesized a series of peptides covering most of this region (Figure 6). These were designed as follows: A (S16-N48), B (P49-N81), C (Y66-K91), D (D97-L123), E (E106-S128) and F (I121-L151).

A representative non-denaturing gel of CaM in the presence of the five different peptides in either 200 μM free Ca^{2+} (Figure 7A) or 1 mM EGTA (Figure 7B) is shown. The peptides alone cannot enter the gel because they are positively charged. CaM bound to

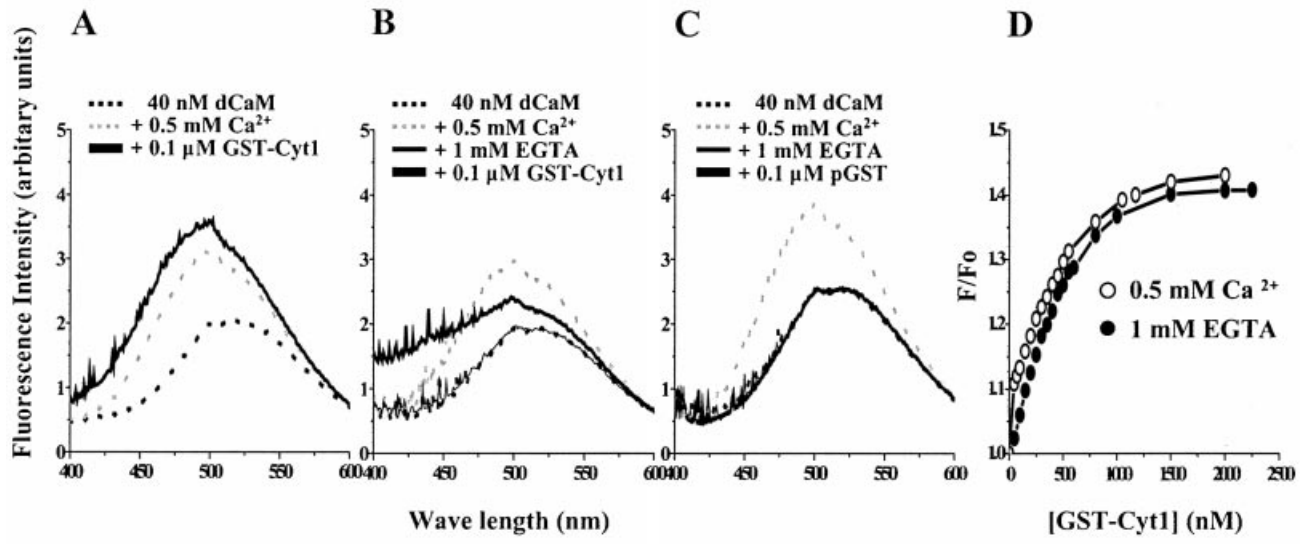

Figure 5 Ca^{2+}-dependent and -independent binding of GST-Cyt1 to dCaM

The emission (λ_{ex} = 340 nm) spectra of 40 nM dCaM were measured in 2 ml of buffer containing 100 μM EGTA. (**A**) Spectra were measured after sequential addition of 0.5 mM Ca^{2+} and 100 nM fusion protein (GST-Cyt1). (**B**), (**C**) Spectra of Ca^{2+}-independent binding of fusion protein to dCaM were measured after sequential addition of 0.5 mM Ca^{2+}, 1 mM EGTA and 100 nM fusion protein GST-Cyt1 or pGST respectively. (**D**) Ca^{2+}-dependent and Ca^{2+}-independent binding curve of GST-Cyt1 to dCaM. Fluorescence change was measured at 500 nm after excitation at 340 nm. *F* represents the fluorescence observed after addition of fusion protein, and F_0 the initial fluorescence of dCaM alone. Curve fitting was done by Microcal™ Origin Version 6.0 and it yielded a K_d value of approx. 0.4 μM.

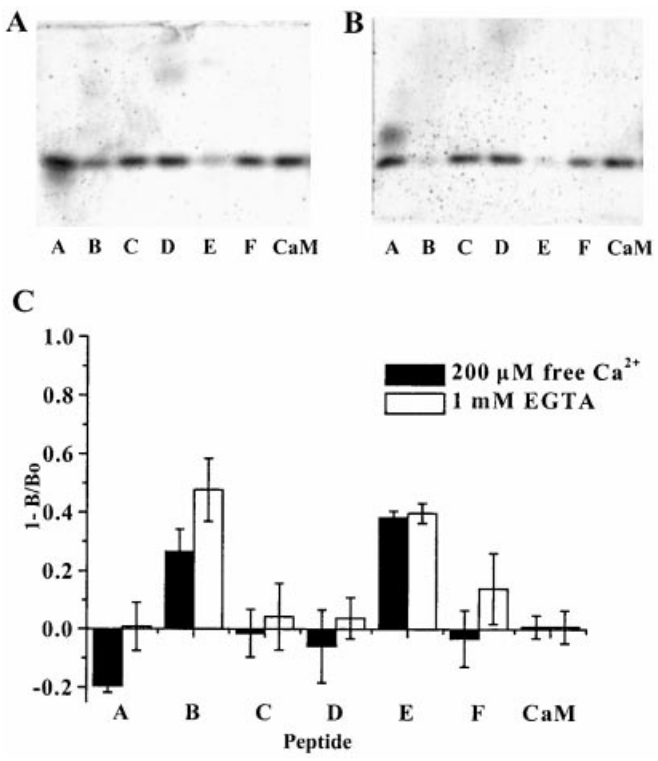

Figure 7 Ability of Ca^{2+}-CaM and apoCaM to bind to IP_3R1 peptides (A–F)

(**A**), (**B**) A representative 15% non-denaturing gel of 3.5 μM CaM in the presence of each of the IP_3R1 peptides (A–F) (105 μM) in a 50 mM Tris buffer (pH 7.4) containing either 200 μM free Ca^{2+} (**A**) or 1 mM EGTA (**B**) stained with SYPRO Orange™. CaM bound to the peptide diminishes the intensity of the CaM band. Lane 1, peptide A (S16-N48); lane 2, peptide B (P49-N81); lane 3, peptide C (Y66-K91); lane 4, peptide D (D97-L123); lane 5, peptide E (E106-S128); lane 6, peptide F (I121-L151) and lane 7, CaM alone. (**C**) Densitometric analysis of the CaM (3.5 μM) bands by ImageQuant 4.2 [25] in the presence of a 30-fold excess of peptide for three independent experiments in the presence of either 200 μM free Ca^{2+} (shaded bars) or 1 mM EGTA (white bars). The vertical axis denotes the intensity loss of the CaM bands after interaction with peptide as compared with CaM alone.

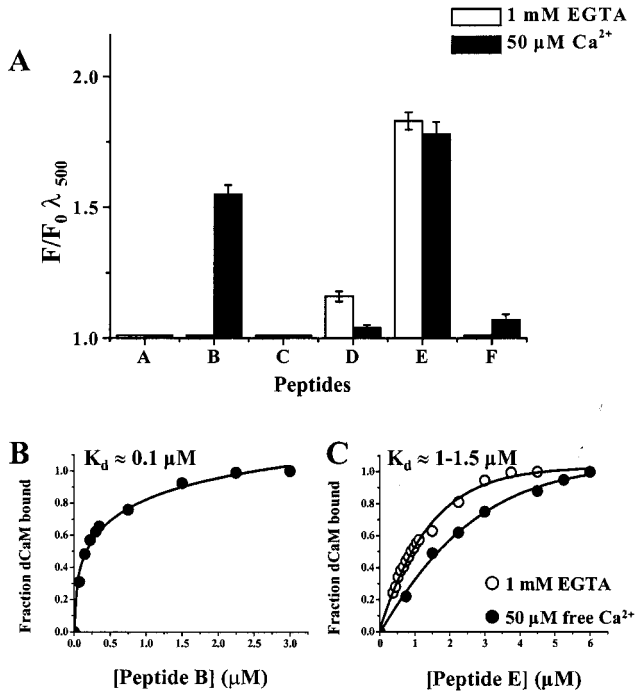

Figure 8 Ca^{2+}-dependent and Ca^{2+}-independent binding of IP_3R1 peptides (A–F) to dCaM

The emission spectra (λ_{ex} = 340 nm) of 40 nm dCaM were measured in 2 ml of buffer containing 100 μM EGTA. (**A**) Increase in dCaM fluorescence emission at λ = 500 nm after addition of 1 μM peptide (A–F) in the presence or absence of Ca^{2+}. Data for each peptide are shown as means ± S.D. (n = 3). (**B**) The Ca^{2+}-dependent CaM-binding curve of peptide B to dCaM. Data in the presence of 50 μM free Ca^{2+} were fitted to a binding curve with $K_d \approx 0.1$ μM. (**C**) The Ca^{2+}-dependent and Ca^{2+}-independent CaM-binding curve of peptide E to dCaM. Data in the presence of 1 mM EGTA were fitted to a binding curve with $K_d \approx 1$ μM. In the presence of 50 μM free Ca^{2+}, the estimated K_d value was approx. 1.5 μM.

peptides B and E, resulting in complexes with those peptides that did not enter the gel. Binding of these peptides to CaM, therefore, diminished the intensity of the CaM band, due to the formation of CaM–peptide complexes. Densitometric analysis of CaM (3.5 μM) bands by ImageQuant 4.2 [25] in the presence of a CaM/peptide molar ratio of 1:30 is summarized for three independent experiments under both conditions in Figure 7(C). The vertical axis in Figure 7(C) denotes the intensity loss of the CaM bands after interaction with a 30-fold excess of peptide as compared with the value for CaM in the absence of peptide. Peptides B and E showed significant binding to both Ca^{2+}-CaM and apoCaM, whereas peptide F showed weak binding. Aberrant results were obtained with peptide A because it was negatively charged under the gel-shift conditions. Gel-shift experiments with CaM1234 were consistent with the observations obtained with CaM (results not shown). Taken together, the gel shifts suggested that the important molecular determinants for CaM binding, both in the presence and absence of Ca^{2+}, were localized within peptides B and E.

Peptide–CaM binding was further quantified in a fluorescence assay using dCaM both in the presence and absence of Ca^{2+}. The vertical axis in Figure 8(A) denotes the fluorescence increase at 500 nm, a measure of the extent of interaction. As shown in Figure 8(A), dCaM displayed a significant interaction with peptide E (E106-S128) both in the presence and absence of Ca^{2+}. The flanking peptides D and F displayed small changes in the absence and presence of Ca^{2+} respectively. In the presence of 50 μM free Ca^{2+}, there was also a significant interaction between dCaM and peptide B (Figure 8A), but surprisingly no interaction was observed in the absence of Ca^{2+}. A possible explanation for this discrepancy could be that the position of the dansyl fluorophores hindered binding between Ca^{2+}-free dCaM and peptide B under these specific conditions. Since such hindrance did not occur for peptide E, these results suggest that both peptides may interact with a different site on dCaM. dCaM did not show interactions with peptides A and C. The affinity was quantified by measuring the fluorescence increase at 500 nm as a function of increasing concentrations of peptide (Figures 8B and 8C). For peptide E, K_d was 1.0 μM in the absence of Ca^{2+}, and 1.5 μM in the presence of 50 μM free Ca^{2+} (Figure 8C). Thus binding between dCaM and the peptide slightly decreased as the free Ca^{2+} concentration increased. This observation is consistent with a site that serves a tethering function. For peptide B, K_d was 0.1 μM in the presence of 50 μM free Ca^{2+} (Figure 8B).

Effect of peptides B and E on the CaM-induced inhibition of IP_3 binding to Lbs-1His

To confirm the involvement of the CaM-binding sites corresponding to peptides B and E in the inhibition of IP_3 binding

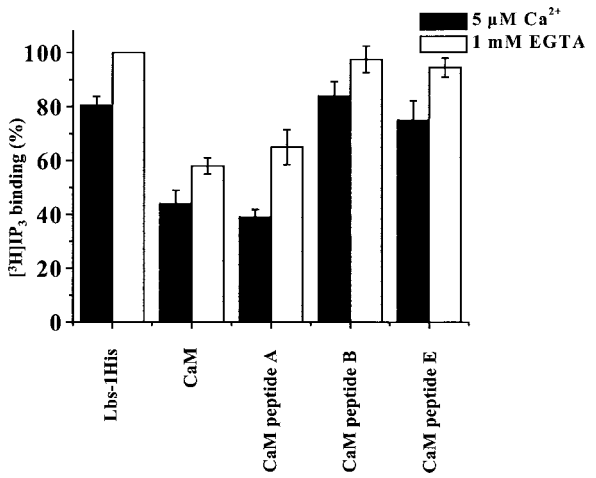

Figure 9 Effect of peptides B and E on the CaM-induced inhibition of IP_3 binding to Lbs-1His

[^{3}H]IP_3 binding to Lbs-1His was measured in the presence of 10 μM CaM either with Ca^{2+} (5 μM, shaded bars) or without Ca^{2+} (1 mM EGTA, white bars) and upon addition of respectively 25 μM peptide A (negative control), peptide B or peptide E. [^{3}H]IP_3 binding was expressed as the percentage of [^{3}H]IP_3 binding in control conditions (Lbs-1His alone; 1 mM EGTA). Binding was measured at pH 7.0 in the presence of 1 mM EGTA and 3.5 nM [^{3}H]IP_3. Data are expressed as the means $\pm$ S.E.M. of at least three independent experiments, each performed in triplicate.

by CaM, we examined whether peptides B and E could reverse the inhibition of IP_3 binding to Lbs-1His caused by CaM. Figure 9 (white bars) shows that addition of either peptide B or peptide E (25 μM) in the presence of CaM (10 μM) fully restored IP_3 binding. In the presence of both Ca^{2+} (5 μM) and CaM (10 μM), peptides B and E counteracted the inhibitory effect caused by CaM, but they did not alter the inhibitory effect caused by Ca^{2+} (Figure 9, shaded bars). No reversal was observed on the addition of peptide A (negative control). These observations suggest that the non-contiguous sequence corresponding to peptides B and E might be a functional Ca^{2+}-independent CaM-binding domain responsible for inhibition of IP_3 binding.

DISCUSSION

It was previously shown that CaM inhibited, in a Ca^{2+}-independent way, IP_3 binding to the native and purified IP_3R as well as to the full-length recombinant type 1 IP_3R [6,7,12–14]. Studies using recombinant ligand-binding domains (first 581 amino acids of IP_3R) also revealed a Ca^{2+}-independent CaM inhibition of IP_3 binding for all IP_3R isoforms [13,15]. The latter studies suggested that a Ca^{2+}-independent interaction site for CaM is present within the N-terminal ligand-binding domain of IP_3R1. This was in agreement with the results of Adkins et al. [7] who obtained evidence for both low-affinity Ca^{2+}-dependent and Ca^{2+}-independent CaM interactions within the first N-terminal 159 amino acids of IP_3R1.

We have measured the effect of Ca^{2+}, CaM and CaM1234 on [^{3}H]IP_3 binding to a recombinant ligand-binding domain (Lbs-1His) and mutants thereof. Ca^{2+} in the absence of CaM inhibited IP_3 binding to Lbs-1His and Lbs-1His mut5 to the same extent, despite the fact that the conserved Ca^{2+}-binding site (Cyt3b, amino acids 378–450) in Lbs-1His mut5 was mutated and could not bind Ca^{2+}. The Cyt3b Ca^{2+}-binding site is apparently not involved in the observed inhibition of IP_3 binding by Ca^{2+}. The possibility that another Ca^{2+}-binding site (Cyt3a, amino acids 304–381) is responsible for the effect of Ca^{2+} is very unlikely, based on the results obtained with deletion mutant Lbs-1His Δ1–225. Deletion of the first 225 amino acids abolished the effects of Ca^{2+} on IP_3 binding, indicating that the Ca^{2+}-interaction site should be located within the N-terminal 125 amino acids, although no known consensus motif for Ca^{2+} binding is present.

CaM (10 μM) in the absence of Ca^{2+} inhibited IP_3 binding to Lbs-1His and Lbs-1His mut5 by approx. 43%. The results obtained for the recombinant ligand-binding domain are in excellent agreement with the maximal inhibition reported for full-length IP_3R1 in Sf9 microsomes (36–40%) [12,13], in rat cerebellum microsomes (36% [6]) and in COS-7 microsomes (35%) [14]. Even IP_3 binding to the $Trp^{1577} \rightarrow Ala$ IP_3R1 mutant was still inhibited by CaM in the absence of Ca^{2+} [14]. The effects of Ca^{2+} (5 μM) and CaM (10 μM) were fully additive and both were absent for Lbs-1His Δ1–225. These results clearly demonstrated that independent interaction sites for Ca^{2+} and for CaM, both of which partially inhibited IP_3 binding, were located in the N-terminal 225 amino acids and outside the IP_3-binding pocket. To demonstrate unequivocally the Ca^{2+}-independent nature of the CaM interaction, we performed similar experiments with CaM1234, a CaM mutant in which the first aspartic acid in each of the four EF-hands was mutated to alanine [29]. The effect of CaM1234 on IP_3 binding was concentration-dependent, and CaM1234 half-maximally inhibited IP_3 binding to Lbs-1His at a concentration of approx. 2 μM. A similar value was found for Lbs-1His mut5. This value is also similar to those reported previously for CaM ($K_d \approx 3$ μM) [6,13]. CaM1234 was a slightly stronger inhibitor of IP_3 binding than CaM and caused a 70% inhibition for Lbs-1His. When both Ca^{2+} and CaM1234 were added, IP_3 binding was further inhibited by up to 82%, indicating that inhibition by CaM1234 was also additive to inhibition by Ca^{2+}. We also observed CaM- and CaM1234-induced inhibition of IP_3 binding for full-length IP_3R1 expressed in Sf9 cells, indicating that the inhibition of IP_3 binding by CaM may be relevant for the functional receptor. Since this Ca^{2+}-independent CaM interaction decreased the IP_3-binding affinity, it is conceivable that such an interaction could modulate the Ca^{2+} regulation and Ca^{2+} gating in an indirect way. Results on the mechanism of channel activation by IP_3 support the view that the sole function of IP_3 is to relieve Ca^{2+} inhibition of the channel [30]. This is also reflected in broadening of the bell-shaped Ca^{2+} curve towards high Ca^{2+} concentrations as more IP_3-binding sites become occupied [31]. In such a model, CaM inhibition of IP_3 binding would result in a more pronounced inhibition of the channel by Ca^{2+}. A physical interaction between the IP_3-binding domain and the channel domain has indeed been demonstrated [32]. The Ca^{2+}-independent inhibition of IP_3 binding by CaM can therefore be compatible with the observation that CaM inhibits IP_3-induced Ca^{2+} release only in the presence of Ca^{2+} [9].

The molecular mechanism for this Ca^{2+}-independent inhibition of IP_3 binding was reflected in the direct interaction of CaM1234 with immobilized GST-Cyt1 (amino acids 1–159 of IP_3R1). GST-Cyt1 bound to CaM1234 both in the presence and absence of Ca^{2+}. Because CaM1234 lacks the ability to act as a Ca^{2+} effector [33,34], this binding can be regarded as a clear indication of a tethering interaction. Estimation of the affinity of the CaM-binding site in GST-Cyt1 using fluorescent CaM revealed a low-affinity binding site ($K_d \approx 0.4$ μM). This value is similar to the value (0.8–1.4 μM) reported using scintillation proximity assay [7]. To map the molecular determinants of the CaM-binding site in GST-Cyt1, we used synthetic peptides representing the N-terminal 159 amino acids of IP_3R1. We demonstrated that both peptides B and E, corresponding to amino acids 49–81 and 106–128 respectively of mouse IP_3R1, bound to both Ca^{2+}-CaM

and Ca^{2+}-free CaM (apoCaM). Peptide B includes a partial IQ (Ile-Gln) motif, whereas peptide E contains both a partial IQ motif and a consensus 1–5–10 CaM-binding motif. The flanking peptides D and F displayed only weak interactions with CaM (both in the gel-shift and the dCaM assay). Since peptide D also contained the consensus 1–5–10 CaM-binding motif but lacked the IQ motif, we conclude that the partial IQ motif in peptide E might be more important as a determinant for binding Ca^{2+}-CaM/apoCaM. It should be pointed out that a pattern search of the complete IP_3R sequence indicated the occurrence of three consensus IQ motifs as well as a large number of partial IQ motifs and Ca^{2+}-dependent CaM-binding motifs (1–5–10 and 1–8–14 motifs). Moreover, not all CaM-binding proteins that bind CaM independently of Ca^{2+} contain an IQ motif [35]. As such, the significance of the partial IQ motifs in peptides B and E remains an open question.

Since both peptides B and E were able to inhibit CaM binding to the recombinant Lbs-1His domain, their sequence may represent a functional CaM-binding domain involved in inhibition of IP_3 binding. Therefore amino acids 49–81 and 106–128 provide a discontinuous tethering site for CaM.

The peptides had a low affinity for Ca^{2+}-independent CaM binding, with a K_d value (0.1–1 μM) comparable with the GST-Cyt1 fusion protein ($K_d \approx 0.4\ \mu$M), the recombinant Lbs-1His domain ($EC_{50} \approx 2\ \mu$M), and the intact IP_3R ($K_d \approx 3\ \mu$M) [6]. Since CaM is present in cells in the 1–10 μM range, and even at higher levels in cerebellum [36], this micromolar affinity may be physiologically relevant. Although the role of apoCaM binding and Ca^{2+}-independent CaM binding is still unknown [37], it is conceivable that the detected Ca^{2+}-independent CaM domain functions as an endogenous attenuator of IP_3R1. It has been reported that the local intracellular availability of CaM and its distribution may change in response to cellular Ca^{2+} or phosphorylation [37,38]. Modulation of the concentration of free CaM itself will determine the occupancy of the Ca^{2+}-independent CaM-binding site and can therefore provide a regulation mechanism. This model is also consistent with the observation that several CaM antagonists cause Ca^{2+} release from the endoplasmic reticulum [39–41], probably by counteracting the tonic inhibition of IP_3Rs by CaM. Alternatively, regulation might be more indirect, based on the finding that CaM-binding sequences have been reported to serve as specific binding motifs for proteins other than CaM [42]. These proteins, such as the recently cloned family of CaM-like Ca^{2+}-binding proteins, may substitute for CaM [43,44] or act as competitors and alter the occupancy of the Ca^{2+}-independent CaM-binding site.

A second model is based on the current thinking about the gating of L-type Ca^{2+} channels [24] and SK potassium channels [29,45], two-ion channels regulated by Ca^{2+} through constitutively bound CaM. CaM tethering to these channels involves two α-helical segments and the effector interaction takes place by recruitment of a third α-helical segment that binds Ca^{2+}-CaM [24]. In the present case, CaM is tethered to peptides B and E, but no effector region was found in the linear neighbouring sequence. Moreover, the functional data presented in the present study clearly demonstrate that Ca^{2+}-bound CaM does not contribute to the inhibitory effect of CaM on IP_3 binding to the recombinant Lbs-1His domain. However, it is possible that the tethering domain that has been detected connects with a Ca^{2+}-CaM-binding site lying elsewhere to allow a fast interaction on stimulation of the cell. This effector site could lie on the IP_3R itself or on accessory proteins such as Ca^{2+}/calmodulin-dependent kinase [46,47], or calcineurin [48]. This model would also be compatible with the observation that CaM inhibits IP_3-induced Ca^{2+} release only in the presence of Ca^{2+} [9].

In conclusion, we have mapped two Ca^{2+}-independent CaM-binding sites in the N-terminal part of IP_3R1. The first one was present between amino acids 49 and 81 and the second one between amino acids 106 and 128. These sequences were identified as components of a discontinuous Ca^{2+}-independent CaM-binding domain and might be responsible for the inhibition of IP_3 binding. Further work is needed to demonstrate the role of these two CaM-binding sites in the functioning of the intact IP_3R1.

We thank Lea Bauwens for her skilful technical assistance. The mammalian CaM cDNA was kindly provided by Dr Z. Grabarek (Boston Biomedical Research Institute, MA, U.S.A.), the rat cDNA for CaM1234 by Dr J. Adelman (Oregon Health and Science University, Portland, OR, U.S.A.) and the p400C1 plasmid containing cDNA of IP_3R1 by Dr K. Mikoshiba and Dr A. Miyawaki (Tokyo, Japan). This work was supported in part by grant 1.5.507.98 from the F.W.O.-Vlaanderen (to I.S.), grant 3.0207.99 from the F.W.O.-Vlaanderen (to H.D.S. and J.B.P.), grant P4/23 from the Program on Interuniversity Poles of Attraction (to J.B.P., G.C., H.D.S. and L.M.) and grant 99/08 from the Concerted Actions of the K. U. Leuven (to L.M., H.D.S., G.C. and J.B.P.). I.S. is supported by the F.W.O.-Vlaanderen with a senior research fellowship.

REFERENCES

1 Balshaw, D. M., Xu, L., Yamaguchi, N., Pasek, D. A. and Meissner, G. (2001) Calmodulin binding and inhibition of cardiac muscle calcium release channel (ryanodine receptor). J. Biol. Chem. **276**, 20144–20153
2 Rodney, G. G., Krol, J., Williams, B., Beckingham, K. and Hamilton, S. L. (2001) The carboxy-terminal calcium binding sites of calmodulin control calmodulin's switch from an activator to an inhibitor of RYR1. Biochemistry **40**, 12430–12435
3 Rodney, G. G., Moore, C. P., Williams, B. Y., Zhang, J. Z., Krol, J., Pedersen, S. E. and Hamilton, S. L. (2001) Calcium binding to calmodulin leads to an N-terminal shift in its binding site on the ryanodine receptor. J. Biol. Chem. **276**, 2069–2074
4 Samso, M. and Wagenknecht, T. (2001) Apocalmodulin and Ca^{2+}-calmodulin bind to neighboring locations on the ryanodine receptor J. Biol. Chem. **277**, 1349–1353
5 Yamaguchi, N., Xin, C. and Meissner, G. (2001) Identification of apocalmodulin and Ca^{2+}-calmodulin regulatory domain in skeletal muscle Ca^{2+} release channel, ryanodine receptor. J. Biol. Chem. **276**, 22579–22585
6 Patel, S., Morris, S. A., Adkins, C. E., O'Beirne, G. and Taylor, C. W. (1997) Ca^{2+}-independent inhibition of inositol trisphosphate receptors by calmodulin: redistribution of calmodulin as a possible means of regulating Ca^{2+} mobilization. Proc. Natl. Acad. Sci. U.S.A. **94**, 11627–11632
7 Adkins, C. E., Morris, S. A., De Smedt, H., Sienaert, I., Torok, K. and Taylor, C. W. (2000) Ca^{2+}-calmodulin inhibits Ca^{2+} release mediated by type-1, -2 and -3 inositol trisphosphate receptors. Biochem. J. **345**, 357–363
8 Hirota, J., Michikawa, T., Natsume, T., Furuichi, T. and Mikoshiba, K. (1999) Calmodulin inhibits inositol 1,4,5-trisphosphate-induced calcium release through the purified and reconstituted inositol 1,4,5-trisphosphate receptor type 1. FEBS Lett. **456**, 322–326
9 Missiaen, L., Parys, J. B., Weidema, A. F., Sipma, H., Vanlingen, S., De Smet, P., Callewaert, G. and De Smedt, H. (1999) The bell-shaped Ca^{2+} dependence of the inositol 1,4,5-trisphosphate-induced Ca^{2+} release is modulated by Ca^{2+}/calmodulin. J. Biol. Chem. **274**, 13748–13751
10 Missiaen, L., De Smedt, H., Bultynck, G., Vanlingen, S., Desmet, P., Callewaert, G. and Parys, J. B. (2000) Calmodulin increases the sensitivity of type 3 inositol-1,4,5-trisphosphate receptors to Ca^{2+} inhibition in human bronchial mucosal cells. Mol. Pharmacol. **57**, 564–567
11 Michikawa, T., Hirota, J., Kawano, S., Hiraoka, M., Yamada, M., Furuichi, T. and Mikoshiba, K. (1999) Calmodulin mediates calcium-dependent inactivation of the cerebellar type 1 inositol 1,4,5-trisphosphate receptor. Neuron **23**, 799–808
12 Cardy, T. J. and Taylor, C. W. (1998) A novel role for calmodulin: Ca^{2+}-independent inhibition of type-1 inositol trisphosphate receptors. Biochem. J. **334**, 447–455
13 Sipma, H., De Smet, P., Sienaert, I., Vanlingen, S., Missiaen, L., Parys, J. B. and De Smedt, H. (1999) Modulation of inositol 1,4,5-trisphosphate binding to the recombinant ligand-binding site of the type-1 inositol 1,4,5-trisphosphate receptor by Ca^{2+} and calmodulin. J. Biol. Chem. **274**, 12157–12162
14 Zhang, X. and Joseph, S. K. (2001) Effect of mutation of a calmodulin binding site on Ca^{2+} regulation of inositol trisphosphate receptors. Biochem. J. **360**, 395–400
15 Vanlingen, S., Sipma, H., De Smet, P., Callewaert, G., Missiaen, L., De Smedt, H. and Parys, J. B. (2000) Ca^{2+} and calmodulin differentially modulate *myo*-inositol 1,4,5-trisphosphate IP_3-binding to the recombinant ligand-binding domains of the various IP_3 receptor isoforms. Biochem. J. **346**, 275–280

16 Yamada, M., Miyawaki, A., Saito, K., Nakajima, T., Yamamoto-Hino, M., Ryo, Y., Furuichi, T. and Mikoshiba, K. (1995) The calmodulin-binding domain in the mouse type 1 inositol 1,4,5-trisphosphate receptor. Biochem. J. **308**, 83–88
17 Islam, M. O., Yoshida, Y., Koga, T., Kojima, M., Kangawa, K. and Imai, S. (1996) Isolation and characterization of vascular smooth muscle inositol 1,4,5-trisphosphate receptor Biochem. J. **316**, 295–302
18 Lin, C., Widjaja, J. and Joseph, S. K. (2000) The interaction of calmodulin with alternatively spliced isoforms of the type-I inositol trisphosphate receptor. J. Biol. Chem. **275**, 2305–2311
19 Sienaert, I., Missiaen, L., De Smedt, H., Parys, J. B., Sipma, H. and Casteels, R. (1997) Molecular and functional evidence for multiple Ca^{2+}-binding domains in the type 1 inositol 1,4,5-trisphosphate receptor. J. Biol. Chem. **272**, 25899–25906
20 Fabiato, A. and Fabiato, F. (1979) Calculator programs for computing the composition of the solutions containing multiple metals and ligands used for experiments in skinned muscle cells. J. Physiol. **75**, 463–505
21 Wawrzynczak, E. J. and Perham, R. N. (1984) Isolation and nucleotide sequence of a cDNA encoding human calmodulin. Biochem Int. **9**, 177–185
22 Lowry, O. H., Rosebrough, N. J., Farr, A. L. and Randall, R. F. (1951) J. Biol. Chem. **193**, 265–275
23 Sienaert, I., De Smedt, H., Parys, J. B., Missiaen, L., Vanlingen, S., Sipma, H. and Casteels, R. (1996) Characterization of a cytosolic and a luminal Ca^{2+} binding site in the type I inositol 1,4,5-trisphosphate receptor. J. Biol. Chem. **271**, 27005–27012
24 Pitt, G. S., Zuhlke, R. D., Hudmon, A., Schulman, H., Reuter, H. and Tsien, R. W. (2001) Molecular basis of calmodulin tethering and Ca^{2+}-dependent inactivation of L-type Ca^{2+} channels. J. Biol. Chem. **276**, 30794–30802
25 Vanlingen, S., Parys, J. B., Missiaen, L., De Smedt, H., Wuytack, F. and Casteels, R. (1997) Distribution of inositol 1,4,5-trisphosphate receptor isoforms, SERCA isoforms and Ca^{2+} binding proteins in RBL-2H3 rat basophilic leukemia cells. Cell Calcium **22**, 475–486
26 Laemmli, U. K. (1970) Cleavage of structural proteins during the assembly of the head of bacteriophage T4v. Nature (London) **227**, 680–685
27 Yoshikawa, F., Morita, M., Monkawa, T., Michikawa, T., Furuichi, T. and Mikoshiba, K. (1996) Mutational analysis of the ligand binding site of the inositol 1,4,5-trisphosphate receptor. J. Biol. Chem. **271**, 18277–18284
28 Kincaid, R. L., Vaughan, M., Osborne, Jr, J. C. and Tkachuk, V. A. (1982) Ca^{2+}-dependent interaction of 5-dimethylaminonaphthalene-1-sulfonyl-calmodulin with cyclic nucleotide phosphodiesterase, calcineurin, and troponin I. J. Biol. Chem. **257**, 10638–10643
29 Xia, X. M., Fakler, B., Rivard, A., Wayman, G., Johnson-Pais, T., Keen, J. E., Ishii, T., Hirschberg, B., Bond, C. T., Lutsenko, S. et al. (1998) Mechanism of calcium gating in small-conductance calcium-activated potassium channels. Nature (London) **395**, 503–507
30 Mak, D. O., McBride, S. and Foskett, J. K. (1998) Inositol 1,4,5-trisphosphate activation of inositol trisphosphate receptor Ca^{2+} channel by ligand tuning of Ca^{2+} inhibition. Proc. Natl. Acad. Sci. U.S.A. **95**, 15821–15825
31 Missiaen, L., De Smedt, H., Parys, J. B., Sienaert, I., Vanlingen, S. and Casteels, R. (1996) Threshold for inositol 1,4,5-trisphosphate action. J. Biol. Chem. **271**, 12287–12293
32 Boehning, D. and Joseph, S. K. (2000) Direct association of ligand-binding and pore domains in homo- and heterotetrameric inositol 1,4,5-trisphosphate receptors. EMBO J. **19**, 5450–5459
33 Zuhlke, R. D., Pitt, G. S., Deisseroth, K., Tsien, R. W. and Reuter, H. (1999) Calmodulin supports both inactivation and facilitation of L-type calcium channels. Nature (London) **399**, 159–162
34 Zuhlke, R. D., Pitt, G. S., Tsien, R. W. and Reuter, H. (2000) Ca^{2+}-sensitive inactivation and facilitation of L-type Ca^{2+} channels both depend on specific amino acid residues in a consensus calmodulin-binding motif in the α1C subunit. J. Biol. Chem. **275**, 21121–21129
35 Rhoads, A. R. and Friedberg, F. (1997) Sequence motifs for calmodulin recognition. FASEB J. **11**, 331–340
36 Kakiuchi, S., Yasuda, S., Yamazaki, R., Teshima, Y., Kanda, K., Kakiuchi, R. and Sobue, K. (1982) Quantitative determinations of calmodulin in the supernatant and particulate fractions of mammalian tissues. J. Biochem. (Tokyo) **92**, 1041–1048
37 Jurado, L. A., Chockalingam, P. S. and Jarrett, H. W. (1999) Apocalmodulin Physiol. Rev. **79**, 661–682
38 Luby-Phelps, K., Hori, M., Phelps, J. M. and Won, D. (1995) Ca^{2+}-regulated dynamic compartmentalization of calmodulin in living smooth muscle cells. J. Biol. Chem. **270**, 21532–21538
39 Wolf, B. A., Colca, J. R. and McDaniel, M. L. (1986) Calmodulin inhibits inositol trisphosphate-induced Ca^{2+} mobilization from the endoplasmic reticulum of islets. Biochem. Biophys. Res. Commun. **141**, 418–425
40 Schlatterer, C. and Schaloske, R. (1996) Calmidazolium leads to an increase in the cytosolic Ca^{2+} concentration in *Dictyostelium discoideum* by induction of Ca^{2+} release from intracellular stores and influx of extracellular Ca^{2+}. Biochem. J. **313**, 661–667
41 Jan, C. R., Yu, C. C. and Huang, J. K. (2000) *N*-(6-aminohexyl)-5-chloro-1-naphthalenesulfonamide hydrochloride) (W-7) causes increases in intracellular free Ca^{2+} levels in bladder female transitional carcinoma (BFTC) cells. Anticancer Res. **20**, 4355–4359
42 Sencer, S., Papineni, R. V., Halling, D. B., Pate, P., Krol, J., Zhang, J. Z. and Hamilton, S. L. (2001) Coupling of RYR1 and L-type calcium channels via calmodulin binding domains. J. Biol. Chem. **276**, 38237–38241
43 Haeseleer, F., Sokal, I., Verlinde, C. L., Erdjument-Bromage, H., Tempst, P., Pronin, A. N., Benovic, J. L., Fariss, R. N. and Palczewski, K. (2000) Five members of a novel Ca^{2+}-binding protein (CABP) subfamily with similarity to calmodulin. J. Biol. Chem. **275**, 1247–1260
44 Sokal, I., Li, N., Verlinde, C. L., Haeseleer, F., Baehr, W. and Palczewski, K. (2000) Ca^{2+}-binding proteins in the retina: from discovery to etiology of human disease 1. Biochim. Biophys. Acta **1498**, 233–251
45 Keen, J. E., Khawaled, R., Farrens, D. L., Neelands, T., Rivard, A., Bond, C. T., Janowsky, A., Fakler, B., Adelman, J. P. and Maylie, J. (1999) Domains responsible for constitutive and Ca^{2+}-dependent interactions between calmodulin and small conductance Ca^{2+}-activated potassium channels. J. Neurosci. **19**, 8830–8838
46 Ferris, C. D., Huganir, R. L., Bredt, D. S., Cameron, A. M. and Snyder, S. H. (1991) Inositol trisphosphate receptor: phosphorylation by protein kinase C and calcium calmodulin-dependent protein kinases in reconstituted lipid vesicles. Proc. Natl. Acad. Sci. U.S.A. **88**, 2232–2235
47 Zhu, D. M., Tekle, E., Chock, P. B. and Huang, C. Y. (1996) Reversible phosphorylation as a controlling factor for sustaining calcium oscillations in HeLa cells: involvement of calmodulin-dependent kinase II and a calyculin A-inhibitable phosphatase. Biochemistry **35**, 7214–7223
48 Cameron, A. M., Steiner, J. P., Roskams, A. J., Ali, S. M., Ronnett, G. V. and Snyder, S. H. (1995) Calcineurin associated with the inositol 1,4,5-trisphosphate receptor-FKBP12 complex modulates Ca^{2+} flux. Cell (Cambridge, Mass.) **83**, 463–472
49 Furuichi, T., Yoshikawa, S. and Mikoshiba, K. (1989) Nucleotide sequence of cDNA encoding P400 protein in the mouse cerebellum. Nucleic Acids Res. **17**, 5385–5386

Received 23 January 2002/18 March 2002; accepted 16 April 2002
Published as BJ Immediate Publication 16 April 2002, DOI 10.1042/BJ20020144